Solid-State Electrochemical Micromachining

Kai Kamada,*,† Kazuyoshi Izawa,‡ Yuko Tsutsumi,‡ Shuichi Yamashita,‡ Naoya Enomoto,† Junichi Hojo,† and Yasumichi Matsumoto‡

Department of Applied Chemistry, Faculty of Engineering, Kyushu University, Fukuoka 812-8581, Japan, and Department of Applied Chemistry and Biochemistry, Faculty of Engineering, Kumamoto University, Kumamoto 860-8555, Japan

Received February 8, 2005
Revised Manuscript Received March 10, 2005

Surface microstructuring of substrates plays a significant role in microelectronics and optoelectronics. The process has recently been extended to the fabrication of chemical systems such as microreactors[1] and micropumps.[2] The textured surfaces are fabricated using one of two general approaches. One is the topographic deposition of desired materials onto the surface.[3] This is the "build-up" type approach, in which the surface is constructed from the molecular or atomic scale. Micromachining belongs to the other category and can be considered to be a "shaving off" type texturing method. Electrochemical micromachining (EM), which works by local dissolution of a conducting substrate (metals, semiconductors) under an applied anodic bias in solution, is one of the most widely used methods because it requires simple equipment and enables more rapid etching than other techniques such as ion beam milling and laser abrasion. However, a liquid electrolyte, which is difficult to handle, is required as a conducting medium between the two electrodes. In addition, high-resolution patterning requires masking. The latter problem is solved by the combined use of position selective laser and ion beam irradiation to draw a minute pattern,[4−6] or the application of an ultrashort voltage pulse.[7−9] In this communication, we propose a simple, novel route for solid-state micromachining using an anodic electrochemical reaction at the microcontact between the ion conducting microelectrode and metal substrate. More concretely, the metal substrate is locally incorporated into the ion conductor in the form of metal ions via the microcontact under a dc bias. The substrate is micromachined as a result of the continuous application of an electric field, which eliminates the need for wet-processing. The present method, which we shall refer to as solid-state electrochemical micromachining (SSEM), can easily control the machining size and depth by adjusting the contact area or other EM parameters. Moreover, scanning the microelectrode under an applied electric field results in a fine-patterned surface. The following sections will focus on the fundamental mechanism behind SSEM and present some experimental results.

The model for ion migration in the SSEM system is depicted in Figure 1a. The β''-Al_2O_3 (typically, Na-β''-Al_2O_3), which conducts a variety of metal ions in the interlayer of spinel blocks, was employed as an ion conductor. The solid-state electrochemical cell consists of an Ag plate (cathode)/pyramid-like Na-β''-Al_2O_3 microelectrode[10]/target metal substrate (thickness: 0.5 mm; M: Ag or Zn; anode) system. To reduce the mechanical stress at the microcontact to a minimum and remain constant, the experimental setup was devised with only the weight of the microelectrode (ca. 0.02 g) to the metal substrate. When a dc electric field is applied to the cell, the local region of the M anode near the solid−solid interface is electrochemically oxidized to M^{n+},[11] which, in turn, is injected into the Na-β''-Al_2O_3 via the microcontact. Na^+ migrates through the β''-Al_2O_3 and is deposited as Na metal at the Ag cathode/Na-β''-Al_2O_3 interface. Na metal immediately reacts with the O_2 and CO_2 in the air to form Na_2CO_3. Thus, the electrolysis mechanism corresponds to the electrochemical substitution of M^{n+} for Na^+ in the β''-Al_2O_3. As a result, the M anode electrochemically dissolves as M^{n+} into β''-Al_2O_3. Since the contact radius at the Na-β''-Al_2O_3/M interface is on the order of 10 μm,[12] a position selective dissolution occurs at the microcontact, and thus SSEM is achieved.

SSEM was carried out under galvanostatic conditions. Figure 2 shows the time dependence of applied voltage during a typical constant-current electrolysis run without (a) and with (b) tracing the β''-Al_2O_3 microelectrode along the surface of the Ag plate. When the microelectrode was fixed on the Ag surface (Figure 2a), the applied voltage gradually decreased except during the initial stage of electrolysis (<20 min). Others have reported that the voltage response in the

* To whom correspondence should be addressed. E-mail: kamada@cstf.kyushu-u.ac.jp.
† Kyushu University.
‡ Kumamoto University.

(1) Wan, Y. S. S.; Chau, J. L. H.; Gavriilidis, A.; Yeung, K. L. *Microporous Mesoporous Mater.* **2001**, *42*, 157.
(2) Xu, D.; Wang, L.; Ding, G. F.; Zhou, Y.; Yu, A. B.; Cai, B. H. *Sens. Actuators* **2001**, *A93*, 87.
(3) Tan, B.; Venkatakrishnan, K.; Tok, K. G. *Appl. Surf. Sci.* **2003**, *207*, 365.
(4) Chauvy, P.-F.; Hoffmann, P.; Landolt, D. *Electrochem. Solid-State Lett.* **2001**, *4*, C31.
(5) Chauvy, P.-F.; Hoffmann, P.; Landolt, D. *Appl. Surf. Sci.* **2003**, *211*, 113.
(6) Teo, E. J.; Breese, M. B. H.; Tavernier, E. P.; Bettiol, A. A.; Watt, F.; Liu, M. H.; Blackwood, D. J. *Appl. Phys. Lett.* **2004**, *84*, 3202.
(7) Schuster, R.; Kirchner, V.; Allongue, P.; Ertl, G. *Science* **2000**, *289*, 98.
(8) Allongue, P.; Jiang, P.; Kirchner, V.; Trimmer, A. L.; Schuster, R. *J. Phys. Chem. B* **2004**, *108*, 14434.
(9) Kirchner, V.; Xia, X.; Schuster, R. *Acc. Chem. Res.* **2001**, *34*, 371.

(10) The commercial Na-β''-Al_2O_3 (diameter: 7 mm; thickness: 2 mm) or a Ag-β''-Al_2O_3 polycrystal was used as an ion conductor. Ag-β''-Al_2O_3 was prepared by ion exchange of Na-β''-Al_2O_3 in a $AgNO_3$ molten salt over 24 h. Complete exchange of Ag for Na was confirmed by electron probe microanalysis (EPMA) in the cross section of β''-Al_2O_3 ceramics after exchange. The obtained β''-Al_2O_3 was polished with emery paper to form a pyramid-like microelectrode as shown in Figure 1b.

(11) Thévenin-Annequin, C.; Levy, M.; Pagnier, T. *Solid State Ionics* **1995**, *80*, 175.

(12) The contact area between the microelectrode and metal substrate in Figure 1a was estimated by scanning electron microscopy (SEM) observation of the surface depressions produced by pressing the microelectrodes onto the metal surface under actual experimental conditions. Assuming a hemispherical microcontact between the microelectrode and the metal, the contact radius was estimated to be on the order of 10 μm. This value was slightly altered by the apex configuration of the hand-polished microelectrode and the processing temperature.

10.1021/cm0502929 CCC: $30.25
Published on Web 03/24/2005

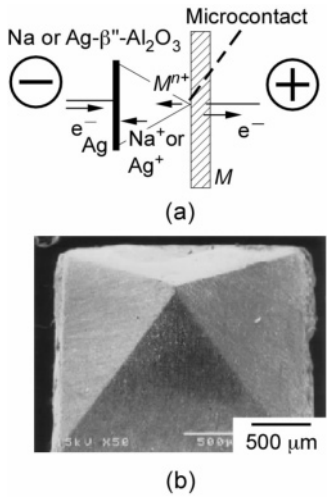

Figure 1. (a) Model for ion migration during SSEM of metal substrate. (b) SEM image of typical β''-Al_2O_3 microelectrode.

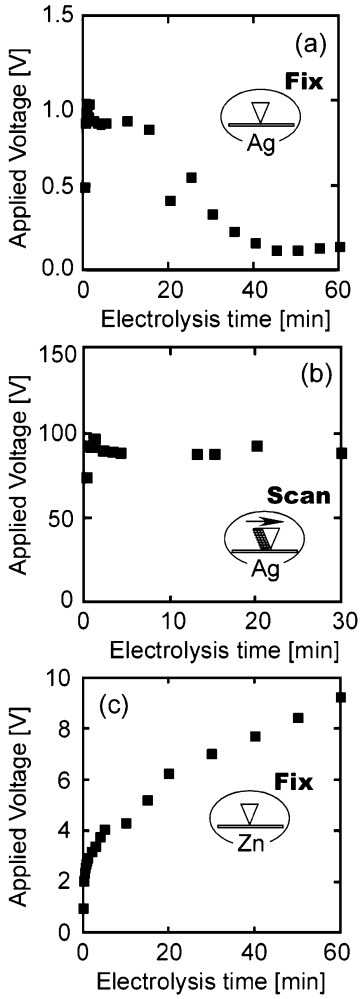

Figure 2. Typical time evolution of applied voltage under constant current electrolysis; (a) Ag micromachining using fixed microelectrode (100 μA, 873 K). (b) Ag micromachining on scanning microelectrode (scan rate: 1 μm/s, 50 μA, 673 K). (c) Zn micromachining using fixed microelectrode at 0.1 μA and 623 K.

ion conducting microelectrode technique depends on the electrical resistance only in the small region near the microcontact[13,14] because the current density at the Ag (cathode)/β''-Al_2O_3 would be negligible compared with that at the microcontact. Taking into account the fact that the type of mobile cations (Na^+ or Ag^+) in β''-Al_2O_3 is independent of the applied voltage, the voltage changes in Figures 2a and 2b seemed to be mainly influenced by the electrochemical reaction at the microcontact (Ag^+/Ag). Thus, the decrease in voltage suggests that the contact area between the pyramid-like microelectrode and Ag plate increased with electrolysis time. That is, the microelectrode was embedded in the Ag anode. By contrast, when the microelectrode was scanned during electrolysis, the applied voltage remained almost constant throughout the duration of electrolysis (Figure 2b), except for some variations that may have been due to the surface roughness or the slight change in temperature. In this case, the contact area of the microcontact was maintained constant, and machining always proceeded on the original Ag surface.

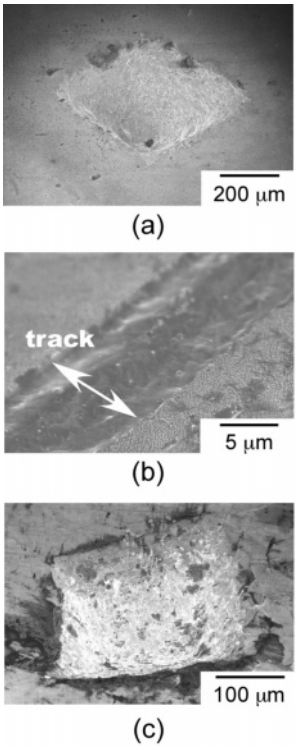

Figure 3. (a) Surface depression of Ag plate after applying 100 μA for 20 min at 873 K using fixed microelectrode. (b) Line-patterned Ag surface under 50 μA at 673 K on scanning microelectrode (1 μm/s). (c) Zn surface after point-machining at 0.1 μA and 623 K for 10 h.

SSEM of the Ag plate was performed using a fixed Na-β''-Al_2O_3 microelectrode. Ag was detected in the cross section of the Na-β''-Al_2O_3 by EPMA measurement after electrolysis. Thus, the ion migration mechanism proposed above actually proceeded during the electrolysis. Figure 3a shows an SEM image[15] of the Ag surface after micromachining under a constant current of 100 μA for 20 min at 873 K. The black dot around the center of the image was the maximum depth position (about 120 μm), which the top of the microelectrode reached just after micromachining.[16] The photograph indicates that the Ag plate was drilled

(13) Wiemhöfer, H.-D. *Ber. Bunsen-Ges. Phys. Chem.* **1993**, *97*, 461.

(14) Zipprich, W.; Waschilewski, S.; Rocholl, F.; Wiemhöfer, H.-D. *Solid State Ionics* **1997**, *101*−*103*, 1015.

(15) To better characterize the surface morphology, all SEM samples were inclining by 35° with respect to the perpendicular electron beam axis.

according to the apex form of the microelectrode, i.e., in the inverse pyramid form. Naturally, the depth was changed by the applied electricity or the microelectrode shape. The quantitative assessment[17] revealed that the current efficiency of the SSEM for the Ag plate (100 μA, 873 K, 1 h) using a fixed Na-β''-Al_2O_3 microelectrode was about 40%. The current loss may be caused by the sparks generated at the inhomogeneous contact between the microelectrode and the metal substrate. Consequently, SSEM was accomplished by using the ion conducting microelectrode. In conventional EM with no masking, the machining size is always larger than that of the counter electrode[18] because of the presence of the electrolyte solution as a conducting medium. On the other hand, since SSEM utilizes direct ion migration via a solid−solid microcontact, the machining dimension is almost identical to the effective contact area. Moreover, Figure 3a suggests that the apex configuration (including the surface roughness) of the microelectrode can be directly transferred to the surface of the work piece.

To groove the Ag plate on a micrometer scale, the Ag-β''-Al_2O_3 microelectrode equipped with an *XYZ* three-dimensional auto stage was scanned along the Ag surface under an electric field. Figure 3b is the SEM image of the Ag surface after scanning the microelectrode in a single direction at 50 μA and 623 K (scan rate: 1 μm/s). The track was produced along the pathway of the microelectrode, and its width and depth were about 10 and 1 μm, respectively. The step observed in the groove may be due to the surface roughness of the sides of the microelectrode. As in the case of a fixed microelectrode, the machining size (width and depth) could be controlled by current and/or scan rate. Since the microelectrode was attached to the automated *XYZ* stage, we could draw various groove patterns on the metal Ag surface, not only simple structures (points and lines) but also more complex forms.

Divalent cations can be substituted into the interlayers of the β''-Al_2O_3 crystal structure alongside the monovalent ions, in which case it behaves as a divalent cation conductor.[19] Thus, a variety of different kinds of metal substrates can presumably be used as a work piece. SSEM of a Zn plate, which supplies the divalent Zn^{2+} and is relatively inert toward surface oxidation at high temperature, was investigated using a fixed Na-β''-Al_2O_3 microelectrode. Figure 2c shows the typical time evolution of applied voltage under a current of 0.1 μA at 623 K below the melting point of zinc (692 K). In contrast to the case of the Ag plate, applied voltage tended to increase monotonically with time, even if the microelectrode was fixed. This may be due to the much lower ionic conductivity of divalent cations (Zn^{2+}) as compared to that of monovalent cations (Na^+) in the β''-Al_2O_3 structure.[20] Figure 3c shows the photograph of a Zn surface after 10 h of SSEM under the same conditions as in Figure 2c. A pyramid-like depression was observed on the Zn surface. This indicates that Zn^{2+} could be removed from Zn metal by using SSEM. A variety of (mono-tetravalent) metal ion conductors have been developed in recent years by many different research groups.[21,22] This means that SSEM can be performed on a whole host of metal substrates, which is an essential merit of the present technique.

Ion conducting microelectrodes have been widely used in the field of solid-state ionics,[23,24] which deals with fast ion conduction in solids. In particular, microelectrodes play an important role in the measurement of local conductivity in ceramic materials[25] and transference numbers in mixed electronic-ionic conductors.[13,14] By contrast, we have used ion conducting microelectrodes as metal source of pinpoint ion doping into solid materials.[26,27] Moreover, it was proved that the microelectrode is an effective tool for the electrochemical patterning of the metal distribution in the surface of or inside glass on a micrometer scale.[28,29] The SSEM method may revolutionize such conventional applications based on novels aspects of the ion conducting microelectrode. SSEM has many advantages over conventional EM. For instance, since it is a solid-state process, no solutions are required, and the metal surface can be directly patterned in almost any configuration desired. SSEM has a number of other merits commonly noted with respect to EM: easy control of machining size and three-dimensional structure by electrochemical parameters and microelectrode configuration. On the other hand, some demerits such as the slow etching rate, the roughness of the machined surface, and the low current efficiency are also found out in the present technique. Therefore, in the future, these problems will soon be solved by advances in electrode fabrication or optimization of electrolysis conditions.

Acknowledgment. The present work was partly supported by a Grant-in-Aid for Scientific Research No. 1576064 from the Ministry of Education, Culture, Sports, Science and Technology, Japan. The authors thank the Center of Advanced Instrumental Analysis, Kyushu University, for the assistance of FE-SEM observations.

CM0502929

(16) The crystal structure and surface morphology of the β''-Al_2O_3 microelectrode were not changed after the SSEM according to the XRD analysis and the SEM observation. However, the β''-Al_2O_3 microelectrode often adhered to the metal substrate after applying high voltage, and its apex broke off the microelectrode in some cases.

(17) The current efficiency of SSEM was calculated from the electric charge and the dissolving amount of Ag in Na-β''-Al_2O_3 using Faraday's law. The amount of Ag existed in Na-β''-Al_2O_3 was measured by ICP after dissolving in aqueous acid solution.

(18) Li, Y.; Zheng, Y.; Yang, G.; Peng, L. *Sens. Actuators* **2003**, *A108*, 144.

(19) Sudworth, J. L.; Tilley, A. R. *The Sodium Sulfur Battery*; Chapman and Hall: New York, 1985.

(20) Farrington, G. C.; Dunn, B. *Solid State Ionics* **1982**, *7*, 267.

(21) Imanaka, N.; Itaya, M.; Ueda, T.; Adachi, G. *Solid State Ionics* **2002**, *154*, 319.

(22) Sakai, N.; Toda, K.; Sato, M. *Electrochemistry* **2000**, *68*, 504.

(23) Fleig, J. *Solid State Ionics* **2003**, *161*, 279.

(24) Fleig, J. *Advances in Electrochemical Science and Engineering*; Wiley-VCH: Weinheim, 2003; Vol. 8.

(25) Fleig, J.; Maier, J. *Phys. Chem. Chem. Phys.* **1999**, *1*, 3315.

(26) Kamada, K.; Udo, S.; Yamashita, S.; Matsumoto, Y. *Solid State Ionics* **2002**, *146*, 387.

(27) Kamada, K.; Udo, S.; Matsumoto, Y. *Electrochem. Solid-State Lett.* **2002**, *5*, J1.

(28) Kamada, K.; Yamashita, S.; Matsumoto, Y. *J. Mater. Chem.* **2003**, *13*, 1265.

(29) Kamada, K.; Yamashita, S.; Matsumoto, Y. *J. Electrochem. Soc.* **2004**, *151*, J33.